RSC Advances

ROYAL SOCIETY OF CHEMISTRY

www.rsc.org/advances

Graphical Abstract

A simple core/shell ZnS:Cu/ZnS QDs based fluorescence enhancement system is constructed for detecting uric acid. The method with high sensitive, selective and lower toxicity features has applied to determination of UA in real samples.

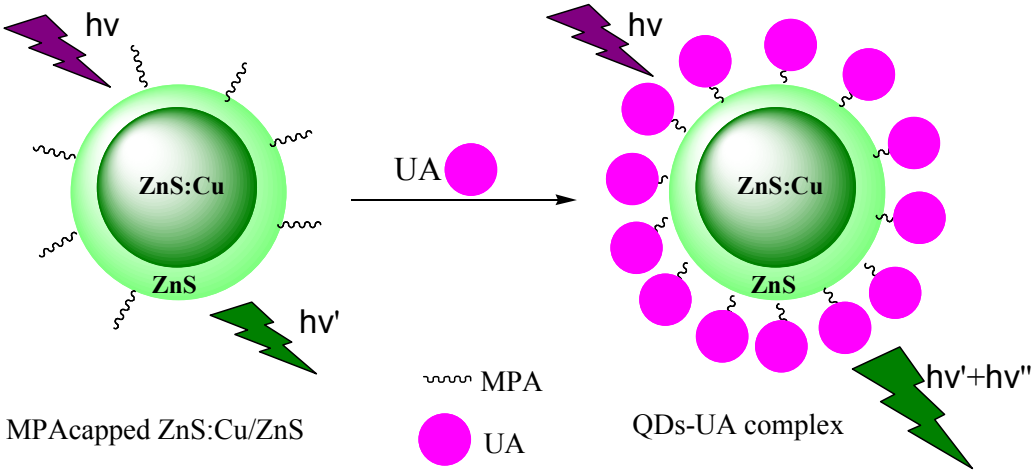

Fluorescence enhancement detection of uric acid based on water-soluble 3-mercaptopropionic acid-capped core/shell ZnS:Cu/ZnS

Meihua Wang, Weifen Niu, Xin Wu, Lixia Li, Jun Yang, Shaomin Shuang* and Chuan Dong*

(*Institute of Environmental Science，College of Chemistry and Chemical Engineering，Shanxi University, Taiyuan, 030006*)

Abstract

3-Mercaptopropionic acid (MPA)-capped ZnS:Cu/ZnS core-shell quantum dots (QDs) have been synthesized via a facile aqueous coprecipitation method and characterized with fluorescence, UV-Vis absorption , infrared spectroscopy and transmission electron microscopy. The fluorescence of ZnS:Cu/ZnS could be increased in the presence of uric acid (UA). The affecting factors for the fluorescence of ZnS:Cu/ZnS were examined including pH, temperature and reacting time. Under the optimized conditions, the fluorescence intensity of the ZnS:Cu/ZnS QDs against the UA concentration showed a linear response in the range of 0.66 μM to 3.3 μM with the correlation coefficient (R^2) 0.9973 and the limit of detection 0.044 μM. Most relevant molecules and physiological ions had no effect on the detection of UA. The feasibility of developed method was further demonstrated by determining the concentration of uric acid in human urine samples and the recoveries were 95%~103%. Our work provides a sensitive, selective and convenient fluorescence method to determine UA in real samples.

* Corresponding Author
Tel.: +86-13934152695; E-mail: dc@sxu.edu.cn

Keywords: Core/shell ZnS:Cu/ZnS; Fluorescence Detection; Uric acid

1 Introduction

Semiconductor nanoparticles or quantum dots (QDs) have emerged as the attractive fluorescent probes for biomolecules detection due to their high fluorescence quantum efficiency, size-dependent broad absorption and readily size-tunable narrow emission as well as photochemical stability. Cadmium chalcogenide QDs hold a special position by virtue of the ease preparation of high-quality samples and the tunability of their luminescence over most of the visible spectrum. Nevertheless, the main concern about the use of fluorophores based on cadmium chalcogenide QDs in biological applications is represented by their inherent toxicity. [1] Hence critical investigations on fabrication of low poisonous or nontoxic QDs are desirable. ZnS QDs are extremely promising candidate with stable luminescence and high quantum efficiency and particularly suitable for use as luminescent host materials for a very large variety of dopants due to their wide band gap energy at room temperature [2]. Numerous metal ions, such as Mn^{2+} [3], Cu^{+} [4], Ag^{+} [5],and Eu^{2+} [6], have been successfully doped into ZnS to produce photoluminescence in different wavelength regions. These doped QDs (d-dots) with minimized self-absorption and higher quantum efficiency can be used as cadmium-free emitters for biolabeling [7], efficient donors for the Förster resonance energy transfer [8] or sensors for biomolecules[9].On the other hand, significant progress has been made on the surface capping ligands of QDs and currently phosphines [10], amines[11], and carboxylic acids [12] are the

most widely used species, through which improved properties and functions can be achieved, such as good biocompatibility and molecular recognition capabilities. The surface modification of QDs with particular capping ligands as the platform makes QDs available for interaction with various target analytes. [13] Therefore, functionlized QDs have been progressed toward different chemical species including ions [14], small molecules [15], and biological macromolecule [16].

Uric acid (UA) is the end product of purine nucleoside, adenosine and guanosine metabolism and is a major antioxidant in humans. Fast and accurate determination of UA level in human physiological fluids has been recognized as a vital clinical indicator in the diagnosis of patients suffering from numerous metabolic disorders such as gout, renal impairment, leukemia, diabetes, and high blood pressure [17]. Different approaches have been involved in the uric acid determination, such as enzymatic-spectrophotometric method [18], electrochemical [20], or fluorescent techniques [21] and capillary electrophoresis [22]. Among them, fluorescence analysis has attracted substantial attention with their unique advantages of simplicity, rapidity, high sensitivity and low cost of instrumentation and maintenance. Ferrer et al. [23] proposed a fluorescent sol-gel biosensor and applied to determine UA in biological fluids. Ren and co-workers [24] reported a new strategy for highly sensitive determination of uric acid based on fluorescence resonance energy transfer (FRET) using gold nanoparticles as energy acceptors. Dey's group [25] synthesized naphthyridine based fluorescent receptors for the recognition of uric acid. To the best of our knowledge, few references were reported based on QDs fluorescence detection

of UA. Zhang et al. [26] found that CdTe quantum dots can act as fluorescence probe for detecting uric acid in biological fluid. We try to use ZnS QDs as the alternative to construct UA detection system toward high sensitivity and low toxicity.

Recently inorganically passivated or core/shell structured QDs have emerged because of their higher-emission quantum efficiency and thermal stability over the single core nanocrystals [27]. A succession of core/shell QDs have been synthesized in aqueous solution, such as ZnSe:Eu/ZnS, CdS:Mn/ZnS, ZnS:Mn/ZnS. However, ZnS:Cu/ZnS core/shell QDs are seldom reported because the different crystal structure between CuS and ZnS led to co-precipitation occur difficultly. Zhang's group [28] firstly synthesized successfully and characterized ZnS:Cu/ZnS core/shell nanocrystals with excellent water-solubility, stability and demonstrated that core/shell structures can be used as a powerful strategy to enhance PL properties of doped semiconductor NCs. This core/shell structure QDs has been employed to determine folic acid in aqueous media [29]. Further extended analytical application of ZnS:Cu/ZnS core-shell quantum dots is desirable.

In this paper, we synthesized ZnS:Cu/ZnS core-shell quantum dots in aqueous solution by using 3-Mercaptopropionic acid (MPA) as the surface-ligand. The polar carboxylic acid group of MPA assembling on the surface of QDs renders the QDs water-soluble and available for interaction with specific analytes. The fluorescence of ZnS:Cu/ZnS QDs were increased dramatically in the presence of UA. The fluorescent detection system of UA was constructed based on core/shell ZnS:Cu/ZnS QDs with high sensitive and selective features and applied to determination of UA in human

urine samples. The results revealed that the as-synthesized ZnS:Cu/ZnS core/shell QDs might be a new promising fluorescence probe for biomedical or clinical analysis.

2 Experimental

2.1. Reagents

All the chemicals were of reagent grade and used without further purification. 3-Mercaptopropionic acid (MPA), sodium sulfide nonahydrate ($Na_2S·9H_2O$), Copper(II) chloride dihydrate ($CuCl_2$), sodium dihydrogen phosphate (NaH_2PO_4) and disodium hydrogen phosphate (Na_2HPO_4), sodium hydroxide (NaOH), heptahydrate zinc sulphate ($ZnSO_4·7H_2O$) and Uric acid (UA) were purchased from Aladdin. Water used throughout was doubly deionized.

2.2. Apparatus

Fluorescence measurements were performed using a Cary Eclipse fluorescence spectrophotometer. UV-Vis absorption spectra were collected using a TU-1901 Double beam UV-Vis spectrophotometer. JEOL JEM-2100 high-resolution transmission electron microscope was adopted to examine the appearance and size of nanoparticles. Infrared spectroscopy was carried out using a FTIR-8400S Infrared spectrometer.

2.3. Methods

2.3.1. Synthesis of ZnS:Cu QDs

MPA-capped ZnS:Cu QDs were synthesized via an aqueous route similar to Yang's method [30] for ZnS:Mn. For 1% copper doping, the synthesis is as follows. In a three-neck round-bottomed flask, 5 mL of 0.1 M $ZnSO_4·7H_2O$, 0.5 mL of 0.01 M

111 $CuCl_2$, and 20 mL of 0.1 M MPA were combined. This solution was diluted to 45 mL
112 with water, and the pH was adjusted to 11 using 1 M NaOH. Next the solution was
113 degassed by bubbling N_2 gas for 30 min, after which 4.5 mL of degassed 0.1 M
114 $Na_2S{\cdot}9H_2O$ was quickly injected into the solution. It remained clear and was stirred
115 for 20 min. The crude solution showed nearly no luminescence. The reaction mixture
116 was then exposed to air and aged 2 h at 50 °C, then The luminescence was observed.
117 The MPA-capped ZnS:Cu QDs could be precipitated by ethanol, the precipitate was
118 centrifuged and washed with ethanol, then dried in vacuum. Stock solutions of
119 $ZnSO_4{\cdot}7H_2O$ and $CuCl_2$ were prepared and used for many syntheses. MPA and
120 $Na_2S{\cdot}9H_2O$ solutions were less stable and prepared fresh each time the synthesis was
121 performed.

122 **2.3.2Synthesis of ZnS:Cu/ZnS QDs**

123 The preparation of ZnS:Cu/ZnS QDs was performed according to Zhang's
124 method [28]with some improvements. The solution after aging was used without
125 purification, and then 8 mL 0.1 M $ZnSO_4{\cdot}7H_2O$/ 5 mL 0.1 M Na_2S/ 17.2 mL 0.1 M
126 MPA/ 2 mL 1 M NaOH were added successively to the solution in 40 times injections
127 with a 30 s interval in between each injection. Then the mixture refluxed for 2 h. After
128 cooling to room temperature the reaction mixture was precipitated with ethanol and
129 centrifuged. The nanocrystals were further washed with ethanol and finally dried
130 under vacuum at room temperature. The obtained powder is white and highly soluble
131 in water.

132 **2.3.3Analytical procedure**

1 mL of 5 mg mL^{-1} ZnS:Cu/ZnS QDs, 2 mL 0.02 M PBS (pH 7.0) were mixed into a 10 mL calibrated test tube, then a certain amount of UA were stepwise added into the mixture and shaken thoroughly for 7 min. At an excitation wavelength of 332 nm, the fluorescence spectra of the mixture were determined in the 380-600 nm emission wavelength range and the fluorescence intensity at 480 nm was used for quantitative analysis.

3. Results and discussion

3.1. Surface characters of ZnS:Cu/ZnS QDs

To identify the conjugation mode between 3-mercaptopropionic acid and ZnS:Cu/ZnS QDs, the IR spectra of the QDs coated by 3-mercaptopropionic acid are measured and compared with pure 3-mercaptopropionic acid. Fig. 1 shows that the spectral features and several peak positions are similar. However, the absorption of S-H stretching vibration at 2600-2500 cm^{-1} has not been found in the IR spectra of ZnS:Cu/ZnS QDs, which demonstrate that the S-H bond in 3-mercaptopropionic acid of the QDs is covalently bound to Zn on the QDs surface.

3.2. HRTEM images of ZnS:Cu and ZnS:Cu/ZnS QDs

High-resolution transmission electron microscopy (HRTEM) is performed to study the morphology of the prepared QDs. Fig. 2 shows the image of the prepared ZnS:Cu and ZnS:Cu/ZnS QDs. The shape of ZnS:Cu QDs is close to spherical and aggregated. After the growth of the ZnS shell, they show no difference with ZnS:Cu QDs except for their average size. Due to the growth of the ZnS shell on ZnS:Cu QDs,

the average size (4.0 nm) of ZnS:Cu/ZnS core/shell QDs is larger than that (2.3 nm) of the ZnS:Cu core QDs. The difference between them means that the shell thickness is around 1.7 nm.

3.3. Spectral characteristics of ZnS:Cu and ZnS:Cu/ZnS QDs

The UV-vis absorption and the fluorescence emission spectra of the ZnS:Cu solution and the ZnS:Cu/ZnS solution are shown in Fig. 3 and Fig.4. Fig.3 shows that the ZnS:Cu solution produces a UV absorption excitonic peak around 280 nm, after 2 h of reflux, the peak is red-shifted to 290 nm. This shift is due to shell growth, which indicate that ZnS shell is coated around the ZnS:Cu core,instead of gathering into a nuclear. Fig. 4 shows that the ZnS:Cu solution develops an emission peak at 474 nm. After ZnS shell is coated around the ZnS:Cu core, the fluorescence intensity increases by almost four times with a very slight shift in emission to 481 nm, which is likely due to surface Cu sites that were not emissive originally become emissive upon incorporation into the ZnS lattice with further ZnS shell growth.

3.4. Optimization of the system

Here, the effect of pH value, reaction temperature and reaction time on the fluorescence intensity of the ZnS:Cu/ZnS QDs–UA mixture was studied in detail.

3.4.1 Effect of pH

The effect of pH on the fluorescence intensity of ZnS:Cu/ZnS QDs and ZnS:Cu/ZnS QDs with 3.3 μM UA was studied in the pH range of 5-10. As shown in

Fig.5, the fluorescence intensity of ZnS:Cu/ZnS QDs and ZnS:Cu/ZnS-UA mixture solution both increased with the change of pH from 5.0 to 8.0. This is due to the protonation of the stabilizer MPA in acid medium. With the increase of pH, the deprotonation of the thiol group in the MPA molecule occurs. This deprotonation could strengthen the covalent bond between Zn and MPA molecule, which could enhance the fluorescence intensity. However, the fluorescence intensity begins to decline with the further increase of pH value, which might be caused by the disintegration of MPA in extreme basic medium. Considering the protonation of the stabilizer MPA in acid medium, and the environment uric acid present, the physiological condition of pH 7.0 PBS was used in further experiments.

3.4.2 Effect of Reaction temperature

The effect of the reaction temperature on the fluorescence intensity of ZnS:Cu/ZnS QDs and ZnS:Cu/ZnS QDs with 3.3 μM UA was studied, and the results were shown in Fig.6. It shows that the fluorescence intensity of the ZnS:Cu/ZnS QDs with 3.3 μM UA is strongest at 25 $^{\circ}$C, then decreased gradually with the increase of reaction temperature from 25 $^{\circ}$C to 50 $^{\circ}$C, which might be caused by the decomposition of UA at high temperature. The fluorescence intensity of the ZnS:Cu/ZnS QDs decreased slightly gradually with the increase of reaction temperature from 20 $^{\circ}$C to 50 $^{\circ}$C. The fluorescence-enhanced extent of the ZnS:Cu/ZnS QDs solution by UA reached a maximum at 25 $^{\circ}$C, so the reaction temperature of 25 $^{\circ}$C was chosen for the further experiments.

199

200 **3.4.3 Effect of Reaction time**

201 The effect of reaction time on the fluorescence intensity of ZnS:Cu/ZnS QDs
202 with 3.3 μM UA was studied and the results were shown in Fig.7. It can be seen that
203 the fluorescence of the QDs increased immediately after the addition of UA, and
204 reached equilibrium after a reaction time of 7min. So in the further study, the mixture
205 of ZnS: Cu/ZnS QDs and UA were shaken thoroughly for 7 min and then the
206 fluorescence intensity was recorded.

207

208 **4. Fluorescence enhancement of MPA-capped ZnS:Cu/ZnS QDs by UA**

209 **4.1. Analytical characteristics**

210 Fig. 8 shows the fluorescence spectra of ZnS:Cu/ZnS QDs upon the addition of
211 different concentrations of UA. It can be seen that the fluorescence intensity of
212 ZnS:Cu/ZnS QDs increased with the UA added. No obvious emission peak shift and
213 change of full width at half maximum were found. The fluorescence enhancing
214 phenomenon might be caused by that after adding uric acid to QDs solutions, the
215 surface of QDs might be changed and cause the decrease of surface defects. Through
216 the formation of hydrogen bond between secondary amine of uric acid and carboxyl
217 of MPA coated on the QDs[26], UA is conjugated to the MPA of nanocrystal surface,
218 such complex will result in the formation of a passivation shell around the nanocrystal,
219 which could remove the surface defects, and the luminescent efficiency will be
220 improved dramatically.

In Fig. 9, it can be seen that the fluorescence intensity of ZnS:Cu/ZnS QDs gradually increased with the addition of UA until 13.2 μM .The insert in Fig.9 illustrates that the fluorescence intensity, $F-F_0$ exhibits a linear relationship with the logarithm of the concentration of uric acid in the range from 0.66 μM to 3.3 μM, which is best described by the equation:

$$F-F_0=-239.30967+368.04448\log C_{UA}(10^{-7}M)$$

F_0 and F are the fluorescence intensity of the ZnS:Cu/ZnS QDs in the absence and presence of uric acid, respectively. The correlation coefficient was 0.9973. The relative standard deviation (RSD) was 1.3 %. The limit of detection (LOD) calculated according to IUPAC definitions is to be 0.044 μM. Table.1 shows the comparison of the established method and other florescence method of UA. The results revealed that the as-conducted system is convenient and sensitive and the ZnS:Cu/ZnS QDs material has lower toxicity over organic fluorescent substances.

4.2 Selectivity study

we studied the effect of a series of physiologically related ions such as K^+, Na^+, NH_4^+, Ca^{2+} and $Mg^{2+}$and other small organic molecules such as ascorbic acid, creatinine, dopamine, urea, glucose, d-lactose and sucrose and some amino acids such as L-alanine, L-cysteine and L-tryptophan on the fluorescence intensity of the ZnS:Cu/ZnS QDs under the same conditions, and the results were shown in Fig. 10. It could be found that the fluorescence intensity of ZnS:Cu/ZnS increases to 2-fold in solution containing 3.3 μM UA, and was almost unaffected by other molecules such as ascorbic acid, dopamine, etc. Therefore, the method has a high selectivity and

could be applied to the direct determination of trace amounts of uric acid in urine samples after dilution.

4.3 Determination of uric acid in human urine

In order to demonstrate the practical utility of the developed system, the prepared method was applied to determine the concentration of uric acid in two human urine samples. To get the appropriate concentration of sample solutions, urine samples are directly diluted with ultrapure water. The results obtained by the standard addition method were shown in Table1, and the accuracy of the proposed method was evaluated by determining the average recoveries of UA in real samples. It can be seen that the RSD was lower than 2.23 % and the average recoveries of UA in the real samples were between 95 % and 103 %. The above results demonstrated the potential applicability of the ZnS:Cu/ZnS QD-based fluorescence probe for the detection of UA in human urine.

5. Conclusion

In summary, we have constructed a core/shell ZnS:Cu/ZnS QDs based fluorescence system for UA and successfully applied to determination of UA levels in human urine. The as-prepared QDs probes for UA detection exhibits highly sensitivity, selectivity and lower toxicity over other QDs systems. To the best of our knowledge, MPA-capped ZnS:Cu/ZnS core/shell QDs was firstly utilized to the determination of uric acid. As a kind of novel fluorescence probe, it is the most favorable alternative.

The present approach extends a new applicable assay for developing economical, sensitive, and selective QD-based fluorescent methods in biomedical or bioprocess.

Acknowledgements

The work is supported by the National Natural Science Foundation of China (No. 21175087, 21175086), Shanxi Province hundred talents program and Shanxi Province personnel returning from overseas fund.

References

[1] D.W. Deng, Y.Q. Chen, J. Cao, J. Tian, Z.Y. Qian, S. Achilefu, Y.Q. Gu, Chem. Mater. 24 (2012) 3029-3037.

[2] C.X. Li, D.Y. Jiang, L.L. Zhang, J.F. Xia, Q. Li, Langmuir. 28 (2012) 9729-9734.

[3] H. Yang, J.Z. Zhao, L.Z. Song, L.C. Shen, Z.C. Wang, L. Wang, D. Zhang, Mater. Lett. 57 (2003) 2287-2291.

[4] X. Tian, L.X. Cao, W. Liu, G. Su, B.h. Dong, Nano. Lett. (7) 2012, 604-607.

[5] W.P. Jian, J.Q. Zhuang, D.W. Zhang, J. Dai, W.S. Yang, Y.B. Bai, Mater. Chem. Phys. 99 (2006) 494-497.

[6] S.C. Qu, W.H. Zhou, F.Q. Liu, N.F. Chen, Z.G. Wang, H.Y. Pan, D.P. Yu, Appl. Phys. Lett. 80 (2002) 3605-3607.

[7] M. Geszke, M. Murias, L. Balan, G. Medjahdi, J. Korczynski,M. Moritz, J. Lulek, R. Schneider, Acta. Mater. 7 (2011) 1327-1338.

[8] S.M. Emin, N. Sogoshi, S. Nakabayashi, T. Fujihara, C.D. Dushkin, J. Phys. Chem. C. 113 (2009) 3998-4007.

[9] L. Dan, H.F. Wang, Anal. Chem. 85 (2013) 4844-4848.

[10] I.L. Medintz, H.T. Uyeda, E.R. Goldman, H. Mattoussi, Nat. Mater. 4 (2005) 435-446.

[11] R.Y. Tu, B.H. Liu, Z.Y. Wang, D.M. Gao, F. Wang, Q.L. Fang, Z.P. Zhang, Anal. Chem. 80 (2008) 3458-3465.

[12] G. M. Duran, A.M. Contentoa, A. Rios, Anal. Chim. Acta. 801 (2013) 84-90.

[13] F. Knittel, E. Gravel, E. Cassette, T. Pons, F. Pillon, B. Dubertret, E. Doris, Nano. Lett. 13 (2013) 5075-5078.

[14] A. Mandal, A. Dandapat, G. De, Analyst, 137 (2012) 765-772.

[15] E.S. Gonzalez, M.T.F. Arguelles, J.M.C. Fernandez, A.S. Medel, Anal. Chim. Acta. 712 (2012) 120-126.

[16] Y.Q. Li, L.Y. Guan, H.L. Zhang, J. Chen, S. Lin, Z.Y. Ma, Y.D. Zhao, Anal. Chem. 83 (2011) 4103-4109.

[17] S.H. Huang, Y.C. Shih, C.Y. Wu, C.J. Yuan, Y.S. Yang, Y.K. Li, T.K. Wu, Biosens. Bioelectron. 19 (2004) 1627-1633.

[18] R.A. Poole, F. Kielar, S.L. Richardson, P.A. Stenson, D. Parker, Chem. Commun. 39 (2006) 4084-4086.

[19] I.A. Rebelo, J.A.P. Piedade, A.M. Oliveira-Brett, Talanta. 63 (2004) 323-331.

[20] A. Babaei, D.J. Garrett, A.J. Downard, Electroanal. 23 (2011) 417-423.

[21] J. Galban, Y. Andreu, M.J. Almenara, S.d. Marcos, J.R. Castillo, Talanta. 54 (2001) 847-854.

[22] J.A. Munoz, M. López-Mesas, M. Valiente, Talanta. 81 (2010) 392-397.

[23] D.M. Perez, M.L. Ferrer, C.R. Mateo, Anal. Biochem. 322 (2003) 238-242.

309 [24] X.Y. Huang, T. Lan, B.C. Zhang, J.C. Ren, Analyst. 137 (2012) 3659-3666.

310 [25] S. Dey, D. Saina, S. Goswami, RSC. Adv. 4 (2014) 428-433.

311 [26] T.L. Zhang, X.Y. Sun, B. Liu, Spectrochim. Acta A. 79 (2011) 1566-1572.

312 [27] H. Yang, P.H. Holloway, G. Cunningham, K.S. Schanze, J. Chem. Phys. 121

313 (2004) 10233-10237.

314 [28] C. Corrado, M. Hawker, G. Livingston, S. Medling, F. Bridges, J. Z. Zhang,

315 Nanoscale. 2 (2010) 1213-1221.

316 [29] M.G. Moritz, G. Clavier, J. Lulek, R. Schneider, J. Lumin. 132 (2012) 987-991.

317 [30] J.Q. Zhuang, X.D. Zhang, G. Wang, D.M. Li, W.S. Yang, T.J. Li, J. Mater. Chem.

318 13(2003) 1853-1857.

319 **Figure captions:**

320 **Table1. The comparison of the established method and other florescence method**

321 **Table2. The determination results of the Human urine samples**

322 **Fig. 1 Infrared spectra of pure 3-mercaptopropionic acid and MPA-coated**

323 **ZnS:Cu/ZnS QDs**

324 **Fig. 2 HRTEM images of ZnS:Cu and ZnS:Cu/ZnS QDs**

325 **Fig. 3 The UV-vis absorption spectra of the ZnS:Cu and the ZnS:Cu/ZnS**

326 **Fig. 4 The fluorescence emission spectra of the ZnS:Cu and the ZnS:Cu/ZnS**

327 **Fig. 5 The effect of pH on the fluorescence intensity of Zn:Cu/ZnS QDs and**

328 **ZnS:Cu/ZnS QDs with 3.3 μM UA**

329 **Fig. 6 The effect of the reaction temperature on the fluorescence intensity of**

330 **ZnS:Cu/ZnS QDs and ZnS:Cu/ZnS QDs with 3.3 μM UA**

Fig. 7 The effect of reaction time on the fluorescence intensity of ZnS:Cu/ZnS QDs with 3.3 μM UA

Fig. 8 The fluorescence spectra of ZnS:Cu/ZnSQDs upon stepwise addition (increments of 2 μL) of a 0.5 mM UA solution in PBS (pH 7.0) buffer solution

Fig. 9 The fluorescence intensity of ZnS:Cu/ZnS QDs with different concentrations of UA. Inset: plot of FL intensity versus logarithm of the concentration of UA in the range of 0.66–3.3 μM. PBS: 0.02 M phosphate buffer solution (pH 7.0).

Fig. 10 Relative fluorescence intensity of ZnS:Cu/ZnS QDs in 0.02 M phosphate buffer solution (pH 7.0) containing various substances (0.033 mM). F and F_0 are the fluorescence intensity in the presence and absence of foreign substances, respectively.

Table1.

Methods	Material	Detection limit	Ref
fluorescent sol-gel biosensor	A coupled uricase–peroxidase system	20nM	[23]
FRET	Gold nanoparticle	25nM	[24]
fluorescence quenching	Naphthyridine	90nM	[25]
fluorescence quenching	CdTe quantum dots	103nM	[26]
Fluorescence enhancement	ZnS:Cu/ZnS	44nM	This work

346 **Table2.**

Samples	Average found /10^{-7}molL^{-1}	Added /10^{-7}molL^{-1}	Total found /10^{-7}molL^{-1}	RSD/ (%) (n=5)	Recovery / (%)
Human urine1	6.81	5	11.97	1.36	103
		15	21.53	1.38	98
Human urine2	6.34	5	11.41	0.64	101
		15	20.58	2.23	95

347 **Fig. 1**

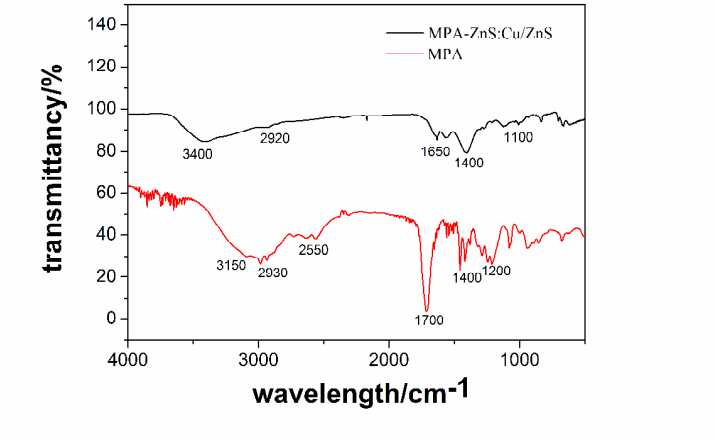

348

349 **Fig. 2**

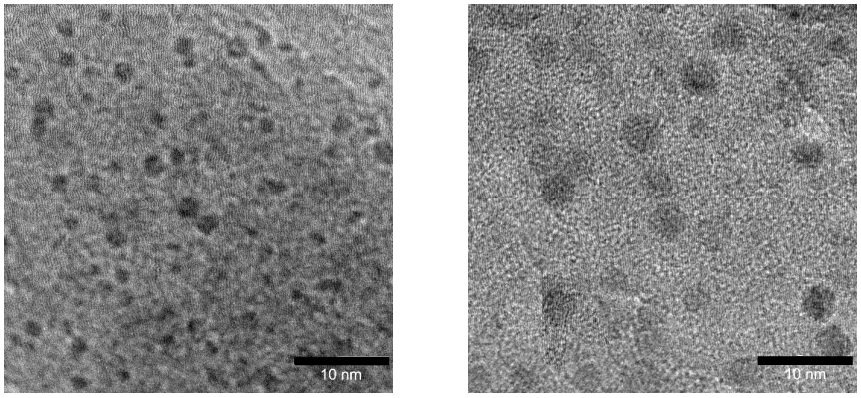

350

351 **a** **b**

352

353

354

355 **Fig. 3**

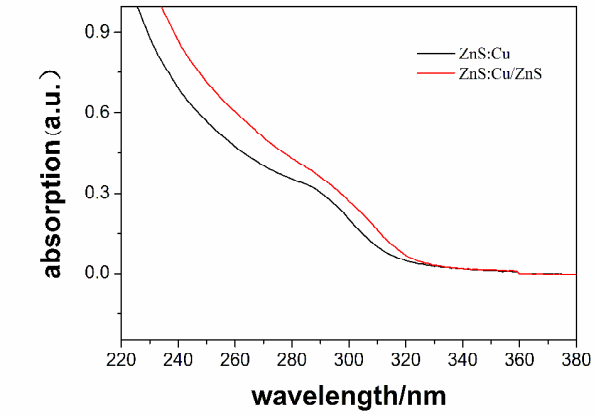

356

357

358 **Fig. 4**

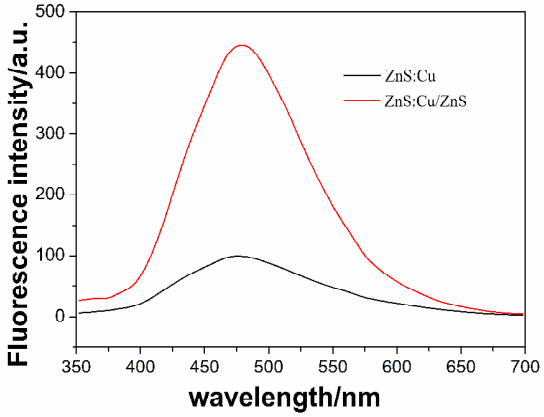

359

360

361

362

363

364

365

366 **Fig. 5**

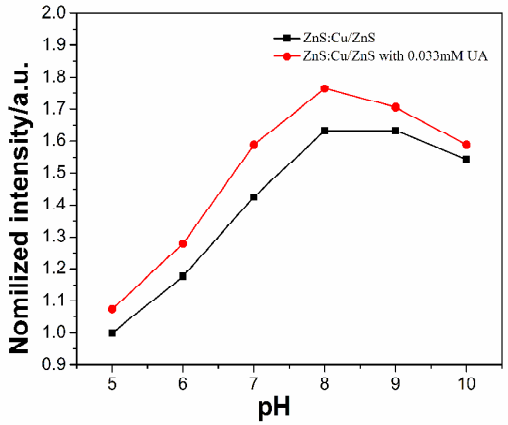

367

368 **Fig. 6**

369

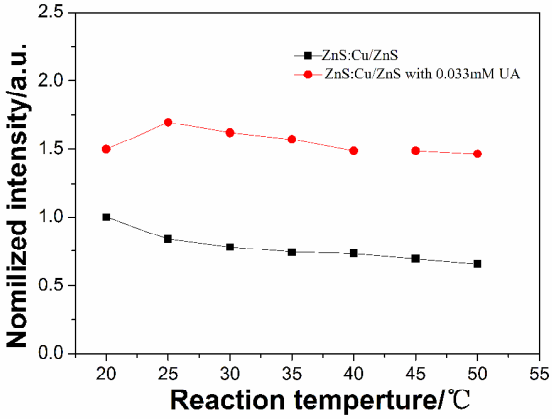

370

371

372

373

374

375

376

377 **Fig. 7**

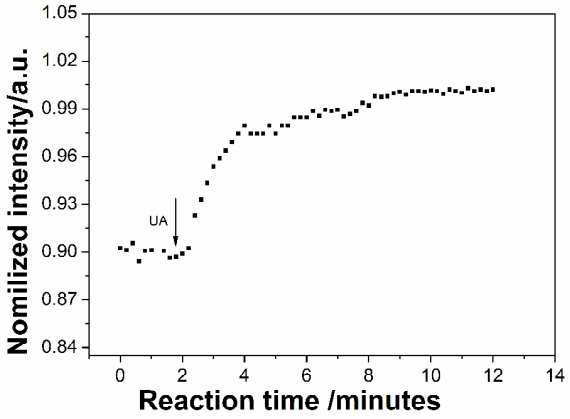

378

379 **Fig. 8**

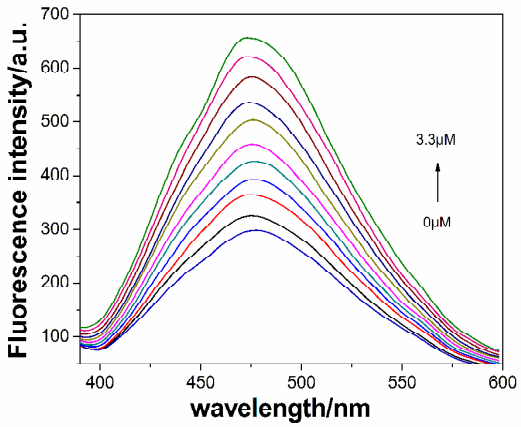

380

381

382

383

384

385

386

387

388 **Fig. 9**

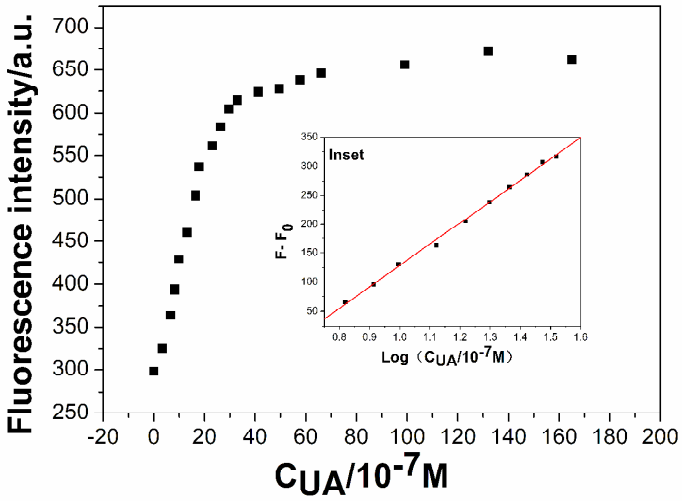

389

390 **Fig. 10**

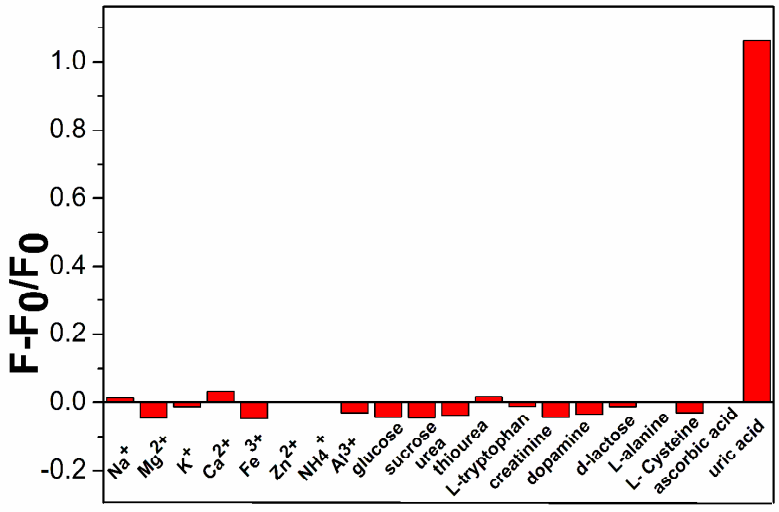

391